2020 5th International Conference on Advanced
Robotics and Mechatronics (ICARM)

Control Strategy for a Developed Robotic Spine Exoskeleton

Farhad Farhadiyadkuri, Lars V. Strøm, Jesper B. Villadsen, Ole H. Hansen, Nicolai S. Sandborg,
Mikkel L. Holm, and Xuping Zhang

***Abstract*— Adolescent Idiopathic Scoliosis, called AIS, estimated to affect up to 4% of adolescents, is the biggest problem among the orthopedic profession. It is an abnormal side-to-side curvature of the spine which occurs between the age of 10 and skeletal maturity without any known reason. Bracing as a common treatment of AIS does not adopt to skeletal changes during the treatment because of its sensor-less design and the lack of control on corrections provided by the brace. Its static design may also affect the patient's safety and convenience. Robotic spine exoskeleton can reduce the problem by restoring the balance of forces along the spine using the measurements received from sensors installed on the robot. In this paper, an in-house developed robotic exoskeleton with one Stewart-Gough Platform (SGP) is designed, and an impedance control strategy is proposed to implement the interaction between the robot and the patient in order to make the exoskeleton more safe and convenient for the patient to use. Besides, an Adaptive Inverse Dynamic Controller (AIDC) is proposed to improve the trajectory tracking of the exoskeleton in the presence of large modeling errors due to uncertain dynamics. Numerical simulations and the validating experimental results are conducted to demonstrate the performance of impedance control in terms of interaction control. In addition, the proper trajectory tracking is verified through the numerical simulations of the proposed AIDC controller.**

I. Introduction

A normal spine has specific curves and the curvatures make the spine have robust and energy-efficient motions, and quick equilibrium management during movement. However, excess body weight, weak muscles, and other forces can result in different types of spine deformity which limit normal activity, impact the quality of life, and can impair respiratory, musculoskeletal, and neurological functions [1], [2]. Three main types of spine deformity are lordosis, kyphosis, and scoliosis. An inward curvature of the lumbar spine and forward curvature of the thoracic spine are called lordosis and kyphosis, respectively. Scoliosis seen in Fig. 1.a, is a three-dimensional disorder of the spine in both the coronal plane and the transverse plane, producing a lateral bend and axial rotation, respectively [3]. Several types of scoliosis exist where the most common form is known as Adolescent Idiopathic Scoliosis (AIS) which has unknown origins and affects up to 4 % of the children between 10 and 16 years of age [4]. This illness forms in the early ages and during growth, and results in pain, lack of movement and reduction in the quality of the patients' life.

F. Farhadiyadkuri, L. V. Strøm, J. B. Villadsen, O. H. Hansen, N. S. Sandborg, and M. L. Holm are research assistants with the Department of Engineering-Robotics, Aarhus University, 8000 Aarhus C.

X. Zhang is an associate professor with the Department of Engineering-Robotics, Aarhus University, 8000 Aarhus C. (Corresponding author, e-mail: xuzh@eng.au.dk)

The most common treatment for AIS, called bracing seen in Fig. 1.b, is a non-adaptive approach to correct abnormal curvatures of the spine and mitigate the need for surgery [5], [6], and [7]. Some braces are designed to apply three-point forces with rotation [8] and [9], while others are designed to provide stretching/traction and rotation to the spine [10]. However, Bracing treatment has some limitations: (i) Excessive prolonged force is known to cause skin breakdown and bone deformation because torso is held in a predefined posture without sensing the force/moments exerted on the torso. (ii) Sensor-less design of braces causes lack of control of the curvature correction and make it difficult to adapt to changes in the torso over the course of treatment [11].

Robotic wearable exoskeletons have been designed to address these limitations by restoring the balance of the forces along the spine. An exoskeleton named Robotic Spine Exoskeleton (RoSE) has been developed by Colombia University, with the ability of controlling the position/orientation of specific cross sections of the human torso while simultaneously measuring the forces/moments exerted on the body. It has also the possibility of controlling the three dimensional forces on the torso while simultaneously measuring the position/orientation of the torso. The Proportional-Integral-Derivative (PID) controller has been used to perform closed-loop control on the desired joint position or joint force [11].

In this paper, a robotic spine exoskeleton is developed in the Robotics Lab at Aarhus University. To move the spine to a specific position and orientation, exoskeleton should be consist of three Stewart Gough Platform (SGP) mounted in series and fixated at the patient's hips, however, we use only one fully functional SGP to demonstrate the control approaches in this preliminary research work. An impedance control is proposed and designed to achieve better interaction between exoskeleton and environment (human torso). Impedance control makes it possible to control the motion and contact force simultaneously by designing a proper interaction between exoskeleton and human torso instead of controlling these variables separately [12]. Besides, in order to make the exoskeleton more adapted to the uncertain dynamics in the dynamic modeling of the SGP, an Adaptive Inverse Dynamic Controller (AIDC) is proposed, where an adaption law is obtained to update the dynamic parameters of the SGP. Both numerical simulations in MATLAB and experimental results demonstrate the proper interaction control of impedance control and numerical simulations using MATLAB indicate that AIDC improves the adaption of physical parameters of

978-1-7281-6479-3/20/$31.00 ©2020 IEEE

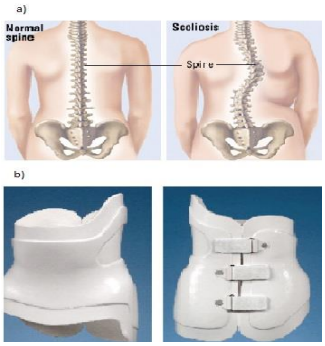

Figure 1. Scoliosis and its common treatment: a) A normal spine and scoliosis, b) Bostone braces

dynamic model and trajectory tracking.

II. Concept Design and System Setup

The purpose of the exoskeleton is to restore the balance of forces along the spine, and the exoskeleton designed in this paper does act as the first prototype for treatment. This exoskeleton centers around the upper thoracic part of the spine, as this region suffers the greatest from the AIS. The mechanical design of the exoskeleton shown in Fig. 2.a consist of three SGPs mounted in series and fixated at the patient's hips. In order to achieve the best fit of the exoskeleton, the SGP is designed based on a surface scan of a single scoliosis patient and is therefore non-symmetric. In this preliminary research work, only one fully functional SGP is made to demonstrate the proposed control strategies, and it is chosen to work with the middle SGP in Fig. 2.a depicted in Fig. 2.b. Note that the lower layer is tilted around the y-axis i.e. β by 19.46° and the upper 23.23° as they are designed to follow the patient's ribs. The workspace requirements for the entire exoskeleton and updated workspace requirements of the SGP of concern are listed in Table I. The values for a single SGP are based on the size of each SGP and coordinated such that the original requirements of entire exoskeleton are met when the three SGPs are combined.

The developed experimental system and data processing setup is described as follows: The mechanical structure of the SGP is manufactured using 3D printing and the interior of the SGP is customized based on a surface scan of the patient affiliated with this research. The actuators' potentiometer feeds back the generalized coordinates q, and the forces induced by the environment on the SGP in the x and y-direction are measured and fed back using force sensors. The input to the SGP is the pulse width modulation (PWM) signal for force control of each actuator, and a National Instruments Compact RIO is utilized for real time control. Using a Host PC, the initial requirements such as the desired change in pose Δx_d, reached in time t_f, and the controller gains K_p and K_d are defined based on the trial and error method. Data processing is split between LabVIEW and MATLAB, where data acquisition and signal processing are performed in LabVIEW, and the system dynamic matrices and the forward kinematic problem are solved continuously using MATLAB on the Host PC. In order to transport data from one program to the other, User Datagram Protocol (UDP) connection is established. LabVIEW and MATLAB run simultaneously and the dynamic matrices estimates $\hat{M}_q, \hat{C}_q$ and $\hat{G}_q$ are updated.

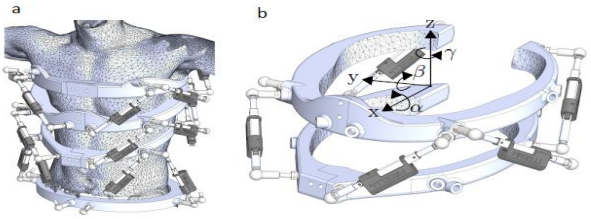

Figure 2. Mechanical design of the exoskeleton. a) CAD-drawing of the exoskeleton mounted on a patient surface scan. b) The SGP of interest in this paper.

TABLE I. WORKSPACE REQUIREMENTS OF ENTIRE EXOSKELETON AND A SINGLE SGP

Movement	Value for entire exoskeleton	Value for a single SGP
Translation in x-direction	-50 to 50 [mm]	-25 to 25 [mm]
Translation in y-direction	-50 to 50 [mm]	-25 to 25 [mm]
Rotation about z-axis, γ	-20° to 20°	-6° to 6°

The actual experimental setup built in the Robotics Lab at Aarhus University is shown in Fig. 3. The setup consists of the following equipment: a Host PC, a wooden test-rig and the SGP which consists of 4 x Actuonix actuators model P16-50-64-12-P, 1 x Actuonix actuator model L12-50-100-12-P, 1 x Firgelli actuator model L12-50-100-12-P, 6 Force Sensing Resistor 402 and a 3D printed interface. Furthermore, the system includes: 3 x Dual H-bridge MDD10A Rev 2.0 used to control the direction of the actuators, an EL302R Power Supply 30V 2A, a National Instruments (NI) cRIO-9082, a NI 9263 Analog Output module, 2 x NI 9201 Analog Input modules and 2 x NI 9472 Digital Output modules.

III. Dynamics

To allow determination of forces in all actuators and joints, various methods exist to perform dynamic analysis such as the Newton-Euler formulation, Virtual-Work formulation, and Lagrange formulation. Using the Newton-Euler formulation the forces in every joint are determined, hence this method is preferable for design purpose and is used in this research. Closed-form dynamic formulation of the SGP is given by:

$$M(X)\ddot{X} + C(X,\dot{X})\dot{X} + G(X) = F \qquad (1)$$

where M denotes the mass and inertia matrix of the SGP as:

$$M(X) = M_P(X) + \sum_{i=1}^{i=6} M_{li}(X) \qquad (2)$$

in which M_P and M_{li} are the mass and inertia matrix of the moving platform and i-th actuator, respectively. The Coriolis and centrifugal matrix of the SGP C is as follows:

Figure 3. The experimental setup showing the developed SGP, the Host PC, and the CompactRIO used for real time control.

$$C(X,\dot{X}) = C_P(X,\dot{X}) + \sum_{i=1}^{i=6} C_{li}(X,\dot{X}) \quad (3)$$

where C_P and C_{li} are the Coriolis and centrifugal matrix of the moving platform and i-th actuator, respectively. The gravity contributions G is:

$$G(X) = G_p(X) + \sum_{i=1}^{i=6} G_{li}(X) \quad (4)$$

where G_p and G_{li} denotes the gravity contributions of the moving platform and i-th actuator, respectively. Besides, F is the wrench force exerted by the manipulator, and $X = \begin{bmatrix} {}^{A}P & {}^{A}O_B \end{bmatrix}^T$, the end-effectors' position and platform orientation as shown in Fig. 2. b and Fig. 4 are given by:

$${}^{A}P = \begin{bmatrix} x & y & z \end{bmatrix}^T, {}^{A}O_B = \begin{bmatrix} \alpha & \beta & \gamma \end{bmatrix}^T \quad (5)$$

where subscript ${}^{A}(\bullet)_B$ indicates that the parameter is taken with respect to frame $\{B\}$ seen from frame $\{A\}$. Note in Fig. 4 that $\{A\}$ denotes the base-frame and $\{B\}$ is the frame of the end-effector. $x, y,$ and z are the end-effectors' position with respect to x, y and z-axes and α, β, and γ are the rotation about x, y and z-axes, respectively. Besides, the velocity and acceleration vectors are given as:

$$\dot{X} = [v_p \quad w_p]^T, \ddot{X} = [\dot{v}_p \quad \dot{w}_p]^T \quad (6)$$

in which v_p and w_p denote the linear and angular velocity of the moving platform, respectively. Also $\dot{v}_p$ and $\dot{w}_p$ denote the linear and angular acceleration of the moving platform respectively.

IV. CONTROLLER DESIGN

In order to control the interaction between manipulator and environment and make the robotic exoskeleton more safe and convenient for the patient to use, impedance control is proposed. In addition, Adaptive Inverse Dynamic Control (AIDC) is designed to compensate the lack of knowledge of the dynamic model of the SGP due to uncertain dynamics.

A. Impedance Control

It is important to design an exoskeleton which is suitable and safe for the patient to wear because it has direct contact with the patient's torso during treatment. Impedance control is proposed to achieve the desirable interaction between manipulator and human torso. The key concept is to model the relationship between the motion and force variables as a dynamic system and control this dynamic relationship to achieve the desirable dynamic interaction between a manipulator and its environment.

The impedance of an electrical circuit is defined as the relation between voltage (effort) and current (flow) which has an analogy connection to the mechanical impedance. For mechanical impedance, the force and velocity are considered as the effort and flow for a single-degree-of-freedom system. For multi-degree-of-freedom systems like SGP, the relation is given by the wrench force applied by the environment F_e (the patient) and motion twist $\dot{X}$. Recall the dynamic formulation of the manipulator in task space in (1) which is extended into:

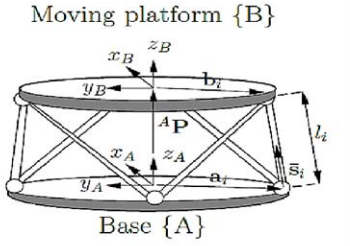

Figure 4. Sketch of a SGP

$$M(X)\ddot{X} + C(X,\dot{X})\dot{X} + G(X) = F + F_e \quad (7)$$

The interaction force produced by the patient is:

$$F_e = M_d(\ddot{X} - \ddot{X}_d) + C_d(\dot{X} - \dot{X}_d) + K_d(X - X_d) \quad (8)$$

where M_d denotes the desired inductive impedance, C_d the desired resistive impedance, and K_d the desired capacitive impedance. In addition, X_d, $\dot{X}_d$, and $\ddot{X}_d$ indicate the desired trajectory, velocity, and acceleration, respectively. Isolating the acceleration yields:

$$\ddot{X} = M_d^{-1}(F_e - C_d(\dot{X} - \dot{X}_d) - K_d(X - X_d)) + \ddot{X}_d \quad (9)$$

Substituting (9) into (7), replacing the system dynamics with estimates denoted $(\hat{\bullet})$, and replacing F_e with the measured contact force at the platform F_m, since exact knowledge of F_e is practically difficult to obtain, the system input force becomes:

$$\begin{aligned} F = {} & (\hat{M}(X)M_d^{-1} - I)F_m + \hat{C}(X,\dot{X})\dot{X} + \hat{G}(X) + \\ & \hat{M}(X)M_d^{-1}(M_d\ddot{X}_d - C_d(\dot{X} - \dot{X}_d) - K_d(X - X_d)) \end{aligned} \quad (10)$$

where $\left(\hat{M}(X)M_d^{-1} - I\right)$ is a matrix weighting of the measured contact force. Substituting (10) into (7) and taking the environmental force into account give:

$$\begin{aligned} & M(X)\ddot{X} + C(X,\dot{X})\dot{X} + G(X) - F_e = \\ & \left(\hat{M}(X)M_d^{-1} - I\right)F_m + \hat{C}(X,\dot{X})\dot{X} + \hat{G}(X) + \\ & \hat{M}(X)M_d^{-1}(M_d\ddot{X}_d - C_d(\dot{X} - \dot{X}_d) - K_d(X - X_d)) \end{aligned} \quad (11)$$

The impedance control architecture is shown in Fig. 5. The required impedance of closed-loop system is set by tuning the desired inductive, resistive and capacitive impedance.

B. Adaptive Inverse Dynamic Control

The main idea of the Inverse Dynamic Control (IDC) is to manipulate the system input in such way the non-linear dynamics is canceled out. The IDC approach was first formulated by Bayo in 1987 where the torque needed to perform a certain task was determined for a multi-link flexible robot manipulator [13]. However, IDC is subject to the stringent requirement of complete knowledge of the dynamic model, which is in reality almost never achievable. An Adaptive Inverse Dynamic Control (AIDC) is presented to achieve a good trajectory tracking in the presence of large modeling error, and it follows the concept presented in [14] and [15]. In this proposed method, dynamic matrices of the system are updated such that the difference between estimates and their true values converges to zero.

In IDC, for linearizing the dynamic model, the wrench force exerted by the manipulator as the controllable variable is designed to be:

$$F = \hat{M}(\ddot{X}_d - K_d\dot{\tilde{X}} - K_p\tilde{X}) + \hat{C}\dot{X} + \hat{G} \quad (12)$$

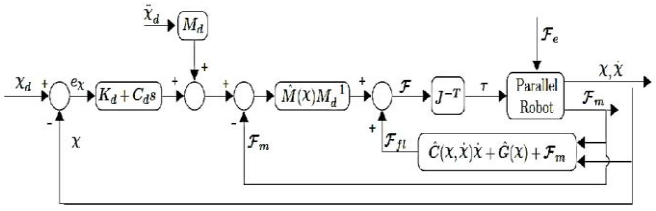

Figure 5. Impedance control architecture in task space.

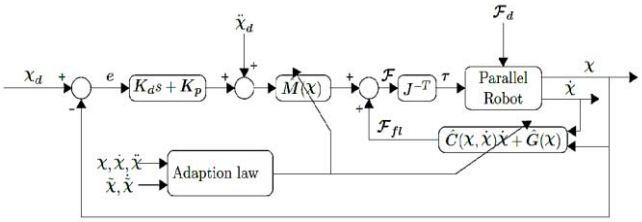

Figure 6. Adaptive Inverse Dynamic Control architecture in task space.

where K_p and K_d are controller gains, $(\bullet)$ denotes the estimate, and $\tilde{X} = X - X_d, \dot{\tilde{X}} = \dot{X} - \dot{X}_d$ are error and its derivative. Substituting the IDC control effort in (12) into the general closed-loop dynamic formulation in (1) yields:

$$M\ddot{X} + C\dot{X} + G(X) = \hat{M}(\ddot{X}_d - K_d\dot{\tilde{X}} - K_p\tilde{X}) + \hat{C}\dot{X} + \hat{G} \tag{13}$$

where $(\tilde{\bullet})$ denotes the mismatch between the estimated value and the true value, thus:

$$\tilde{M} = \hat{M} - M, \tilde{C} = \hat{C} - C, \tilde{G} = \hat{G} - G \tag{14}$$

Add and subtract $\ddot{X}$ into the parenthesis in (13), and simplify to:

$$\tilde{M}\ddot{X} + \tilde{C}\dot{X} + \tilde{G} = \hat{M}(\ddot{\tilde{X}} + K_d\dot{\tilde{X}} + K_p\tilde{X}) \tag{15}$$

which implies that:

$$\ddot{\tilde{X}}_d + K_d\dot{\tilde{X}} + K_p\tilde{X} = \hat{M}^{-1}(\tilde{M}\ddot{X} + \tilde{C}\dot{X} + \tilde{G}) = \hat{M}^{-1}y(X,\dot{X},\ddot{X})\tilde{\theta} \tag{16}$$

where $y(X,\dot{X},\ddot{X})$ is a regression model and $\tilde{\theta}$ a parameter vector of the dynamic model of the SGP. A schematic of the control architecture is seen in Fig. 6.

In order to address stability and obtain stable adaption law, (16) is written in error state space form with the error state space vector:

$$e = \begin{bmatrix} \tilde{X} \\ \dot{\tilde{X}} \end{bmatrix} \tag{17}$$

thus error state space representation is given:

$$\dot{e} = Ae + B\Phi\tilde{\theta}$$
$$A = \begin{bmatrix} 0_{6\times6} & I_{6\times6} \\ -K_{p6\times6} & -K_{d6\times6} \end{bmatrix}, B = \begin{bmatrix} 0_{6\times6} \\ I_{6\times6} \end{bmatrix} \tag{18}$$
$$\Phi = \hat{M}^{-1}y(X,\dot{X},\ddot{X})$$

To ensure stable error dynamics, proportional-derivative gains K_d *and* K_p must be chosen such that the linear part of (18) remains stable, i.e. A becomes Hurwitz. Moreover, the adaption law in the nonlinear part $B\Phi\tilde{\theta}$ should be designed such that tracking error remains globally asymptotically stable, so the adaption law must satisfy the Lyapunov global asymptotic stability theorem. Consider the following Lyapunov candidate function:

$$V = e^T Pe + \tilde{\theta}^T \Gamma\tilde{\theta} \tag{19}$$

where Γ is the learning rate and a constant symmetric positive definite matrix. Following the Lyapunov theorem, the candidate derivative must be negative along any arbitrary trajectory, thus:

$$\dot{V} = e^T(A^TP + PA)e + 2\tilde{\theta}^T\Phi^TB^TPe + 2\tilde{\theta}^T\Gamma\dot{\tilde{\theta}} = -e^TQe + 2\tilde{\theta}^T(\Phi^TB^TPe + \Gamma\dot{\tilde{\theta}}) \tag{20}$$

The first term of $\dot{V}$ is clearly negative definite and by following adaption law:

$$\dot{\hat{\theta}} = -\Gamma^{-1}\Phi^TB^TPe \tag{21}$$

where $\dot{\tilde{\theta}} = \dot{\hat{\theta}}$, the second term vanishes and global asymptotic stability of the error dynamics is ensured:

$$\dot{V} = -e^TQe < 0 \tag{22}$$

Because of using actual position, velocity and accelerations, regression matrix should be computed on-line. In [16] it is shown that by using desired position, velocity and accelerations instead i.e. $y(X_d,\dot{X}_d,\ddot{X}_d)$ yields good trajectory tracking which only relies on off-line calculations and therefore of lower computational complexity. The modified controller uses the same adaption law and its stability analysis follows the same lines as presented above.

V. NUMERICAL SIMULATIONS AND EXPERIMENTS

In this section, the performance of impedance control is compared with the LQR approach in terms of interaction control by means of the numerical simulations and experiments using developed robotic exoskeleton, and adaption of dynamic parameters in AIDC is demonstrated by means of numerical simulations using MATLAB.

A. Evaluation of Impedance Control

The performance of impedance control is verified in terms of comfortable and secure motion of the manipulator when interacting with a stiff environment by numerical simulations using MATLAB at first. The manipulator is simulated to follow a trajectory where an obstacle is placed in its path at the position (-5,-10) mm of xy-plane and collision happens at t=7.5s. The obstacle has stiffness $K_o = 14000I_{6\times6}$ and damping $C_o = 100I_{6\times6}$, which are set arbitrary, and the manipulator's desired stiffness, damping, and mass/inertia are denoted $K_d = 5000I_{6\times6}$, $C_d = 100I_{6\times6}$, and $M_d = 1I_{6\times6}$. Using impedance control the system is modeled as a virtual spring-mass-damper system and the desired parameters are chosen such that the controller is critically damped.

The Linear Quadratic Regulator (LQR) controller is used as a benchmark. It was proposed by R. E. Kalman in 1960 concerns minimizing a cost function for optimizing the performance of the system by tuning the controller gains [17]. Position and orientation error of the moving platform using LQR and impedance control are shown in Fig. 7 and Fig.8, respectively. It is seen that no position and orientation error

occurs before collision and the impedance control have smooth trajectory tracking rather than unstable behavior of the LQR after collision. The wrench forces applied to the patient by the two controllers are also shown in Fig. 9. After collision, the LQR controller becomes unstable and applies rapid impulses to the patient in order to correct the error, where the impedance controller applies a smooth and continuous force, which feels less unpleasant for the patient.

Secondly, the experiment of performing a movement of the end-effector in the y -direction while a stiff object is placed in its way is performed to validate the interaction control of impedance control. To mimic a human torso, a wooden test-rig attached to the base by spring is used and a piece of foam is placed at the interaction points to mimic the skin and underlying tissue of a human and to safeguard the equipment. The test-rig and the manipulator are in contact at the Force Sensitivity Resistor (FSR) locations from the beginning of the test. The results are compared with an identical test run using the LQR controller. The impedance controller parameters used are $M_d = 2, K_d = 10000$, and $C_d = 100$, and the controller gains used in the LQR approach are $K_p = 7244.69$ and $K_d = 1106.22$.

Pose error of the manipulator and forces produced by the controllers are shown in Fig. 10 and Fig. 11. Notice in Fig. 10 that the LQR controller performs the best job of trajectory tracking, however investigating the actuator and wrench forces shown in Fig. 11 reveals the ability of interaction control of the impedance controller and the lack of such by the LQR controller. The actuator forces produced by the LQR are seen

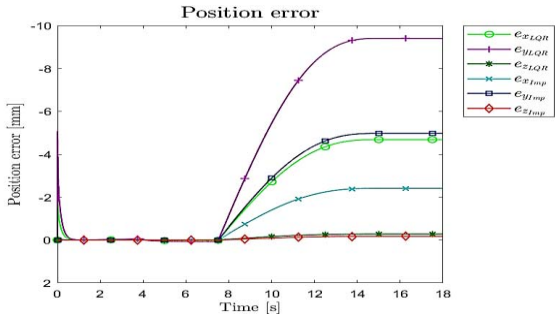

Figure 7. Position error through the simulation with LQR and impedance control

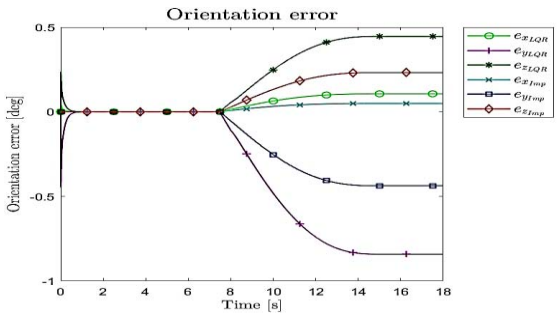

Figure 8. Orientation error through the simulation with LQR and impedance control

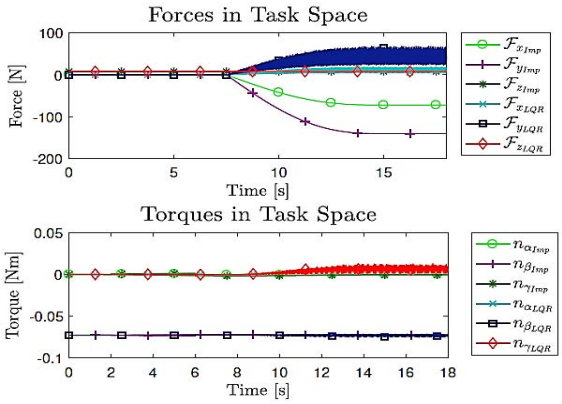

Figure 9. Task space forces with LQR and impedance control

to chatter and change rapidly, which results in an unpleasant assessment for the patient. Also a better performance of the impedance controller in terms of trajectory tracking is achievable by choosing proper desired virtual system dynamics i.e. K_d , C_d , and M_d .

B. *Evaluation of AIDC*

The main purpose of the AIDC is to adapt the physical parameters of the dynamic model to improve the trajectory tracking, and it is verified using numerical simulations in MATLAB. The parameter vector is given:

$$\tilde{\theta} = \begin{bmatrix} m_p & I_{pxx} & I_{pyy} & I_{pzz} & m_{cylinder} & m_{piston} & I_{\lim b_{xx}} \end{bmatrix}^T \quad (23)$$

where $(\bullet)_p$ denotes the moving platform, I inertias, and m masses. The regression model $y(X_d, \dot{X}_d, \ddot{X}_d)$ is derived from the dynamic formulation established in section III for the moving platform and limbs:

$$\begin{aligned} y_p(X_d, \dot{X}_d, \ddot{X}_d) &= Y_{M_p} + Y_{C_p} + Y_{G_p} \\ y_i(X_d, \dot{X}_d, \ddot{X}_d) &= Y_{M_i} + Y_{C_i} + Y_{G_i} \\ y(X_d, \dot{X}_d, \ddot{X}_d) &= \begin{bmatrix} y_p, y_1, y_2, y_3, y_4, y_5, y_6 \end{bmatrix} \end{aligned} \quad (24)$$

where y_p and y_i are respect to the regression model of moving platform and i-th limb, respectively. Besides, the subscripts M, C, and G are respect to the inertia, centrifugal and Coriolis, and gravity terms, respectively. The position and orientation errors over time in the presence of an initial 40% perturbation on parameters are shown in Fig. 12. It is chosen not to adapt on inertias since it has minor influence on the behavior as the desired motion is linear [18]. The controller parameters used in the simulation are $K_p = I_{6\times6}, K_d = I_{6\times6}$, and $\Gamma = diag(35,0,0,0,0.05,0.05,0)$. The adaption rate Γ is set to zero for the inertias as they are not adapted.

Note that the trajectory tracking of the AIDC initially yields poor performance, but continuously, improves through adaption of θ -parameters. Error on adapted θ -parameters is shown in Table II. Good adaption of the moving platform mass and cylinders is achieved, however, the mass of the pistons are not adapted. Since good tracking performance is achieved, this reveals that the mass of the pistons has minimal influence on the manipulator dynamics.

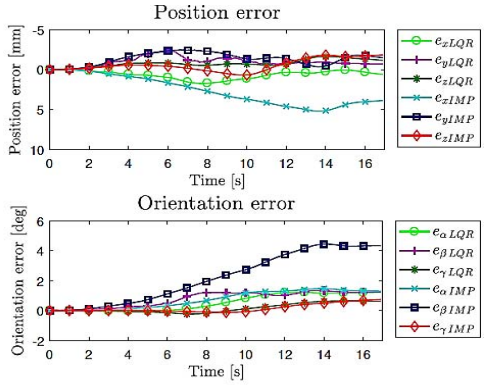

Figure 10. Poseition and orientation error using LQR and impedance control when interacting with a stiff environment.

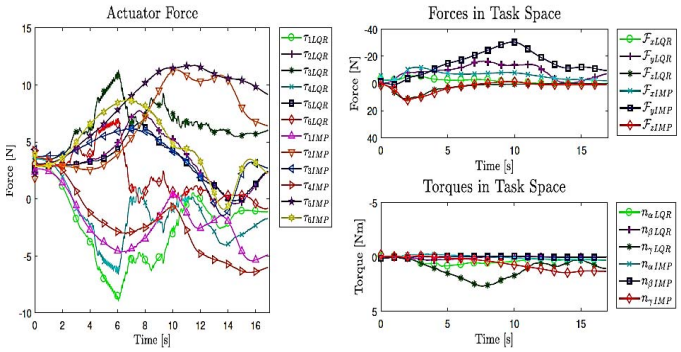

Figure 11. Forces produced by LQR and impedance control when interacting with a stiff environment.

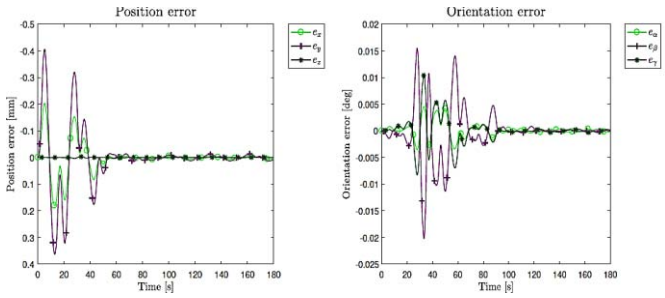

Figure 12. Position and orientation error using AIDC in the presence of 40% perturbation aplied on the parameters.

TABLE II. ERROR ON ADAPTED PARAMETERS WITH INITIAL 40% PERTURBATION

Description	Exact mass (kg)	Adapted mass (kg)	Adapted error (%)
m_p	0.502	0.516	3%
m_{piston}	0.0475	0.0280	41%
$m_{cylinder}$	0.0475	0.0481	1%

VI. CONCLUSION

This paper is mainly concerned with the control strategy of a robotic nonlinear six-DOF Stewart-Gough platform. The robotic SGP system has been developed and built in the Robotics Lab at Aarhus University. Impedance control has been derived and implemented in MATLAB and experimentally tested on the developed robotic SGP. Numerical simulations have been validated with experiments. Both numerical and experimental results have demonstrated the stable interaction control when the robot collides with a stiff object. Besides, an adaptive inverse dynamic control has been presented and implemented in MATLAB simulations to compensate the uncertain dynamics of the SGP by employing an adaption law to update the dynamic model parameters. For improving the interaction control of the impedance control, our ongoing research will consists of: 1) manufacturing a ballistic torso and developing a proper model of the human body, possibly by applying an adaption scheme; 2) extending to three moving platforms from current one moving platform.

REFERENCES

[1] S. Weinstein, L. Dolan, J. C. Cheng, A. Danielsson, and J. A. Morcuende, "Adolescent idiopathic scoliosis," *Lancet,* vol. 371, pp. 1527-1537, 2008.

[2] C. Nnadi and J. Fairback, "Scoliosis: a review," *Pediatrics and Child Health,* vol. 20, no. 5, pp. 215-220, 2009.

[3] P. A. Millner and R. A. Dickson, "Idiopathic Scoliosis: Biomechanics and Biology," *European Spine J,* vol. 5, pp. 362-372, 1996.

[4] S. W. Suh, H. N. Modi, and J. H. Hong, "Idiopathic scoliosis in Korean schoolchldren: a porspective screening study of over 1 million children," *European Spine J,* vol. 20, pp. 1087-1094, 2011.

[5] J. Carlson, "Clinical biomechanics of orthotic treatment of idiopathic scoliosis," *Journal of Prosthetics and Orthotics,* vol. 15, no. 4, 2003.

[6] R. Heary, C. Bono, and S. Kumar, "Bracing for scoliosis," *Neurosurgery,* vol. 63, pp. A125-A130, 2008.

[7] S. Weinstein, L. Dolan, J. Wright, and M. Dobbs, "Effects of bracing in adolescents with idiopathic scoliosis," *New England Journal of Medicine,* vol. 369, no. 16, pp. 1512-1521, 2013.

[8] J. Wynne, "The boston brace system philosophy, biomechanics, design and fit," *Studies in health technology and informatics,* vol. 135, pp. 370-384, 2007.

[9] M. Rigo and H. Weiss, "The cheneau concept of bracing biomechanical aspects," *Studies in Health Technology and Informatics,* vol. 135, pp. 303-319, 2008.

[10] W. P. Blount, "The milwaukee brace in the treatment of the young child with scoliosis," *Archives of Orthopedic and Trauma Surgery,* vol. 56, no. 4, pp. 363-369, 1964.

[11] J. Park, P. R. Stegall, D. P. Roye, and S. K. Agrawal, "Robotic Spine Exoskeleton (RoSE): characterizing the 3-D stiffness of the human torso in the treatment of spine deformity," *IEEE Transactions on Neural Systems and Rehabilitation Engineering,* vol. 26, no. 5, pp. 1026-1035, 2018.

[12] P. Song, Y. Yu, and X. Zhang, "A tutorial survey and comparison of impedance control on robotic manipulation," *Robotica,* vol. 37, no. 5, pp. 801-836. 2019.

[13] E. Bayo, "A finite element approach to control the end-point motion of a single link flexible robot," *Journal of Robotics Systems,* vol. 4, pp. 63-75, 1987.

[14] N. Sadegh and R. Horowitz, "Stability analysis of an adaptive controller for robotic manipulator," *1987 International Conference on Robotics and Automotion*, 1987, pp. 1223-1229.

[15] J. Slotine and W. Li, "On the adaptive control of robot manipulators," *The International Journal of Robotics Research,* vol. 6, no. 3, pp. 49-59, 1986.

[16] N. Sadegh and R. Horowitz, "Stability and robustness analysis of a class of adaptive controllers for robotic manipulators," *The International Journal of Robotics Research,* vol. 9, no. 3, pp. 74-93, 1990.

[17] R. E. Kalman, "On the general theory of control systems," *IFAC Proceedings Volumes,* vol. 1, no. 1, pp. 491-502, 1960.

[18] M. Honegger, A. Codourey, and E. Burdet, "Adaptive control of the Hexaglide, a 6 dof parallel manipulator," *Proceedings of International Conference on Robotics and Automation,* 1997, pp. 543-548.